NJC

Accepted Manuscript

This is an *Accepted Manuscript*, which has been through the Royal Society of Chemistry peer review process and has been accepted for publication.

Accepted Manuscripts are published online shortly after acceptance, before technical editing, formatting and proof reading. Using this free service, authors can make their results available to the community, in citable form, before we publish the edited article. We will replace this *Accepted Manuscript* with the edited and formatted *Advance Article* as soon as it is available.

You can find more information about *Accepted Manuscripts* in the Information for Authors.

Please note that technical editing may introduce minor changes to the text and/or graphics, which may alter content. The journal's standard Terms & Conditions and the Ethical guidelines still apply. In no event shall the Royal Society of Chemistry be held responsible for any errors or omissions in this *Accepted Manuscript* or any consequences arising from the use of any information it contains.

ROYAL SOCIETY OF CHEMISTRY

www.rsc.org/njc

Facile fabrication of OA-POSS modified near-infrared-emitting CdSeTe alloyed quantum dots and its bioapplication

Xue Zhao[a], Weijia Zhang[a], Yongzhong Wu[a]*, Hongzhi Liu[b], Xiaopeng Hao[a]*

[a]State Key Laboratory of Crystal Materials, Shandong University, 27 Shandanan Road, Jinan 250100, P. R. China. E-mail: wuyz@sdu.edu.cn; xphao@sdu.edu.cn

[b]Key Laboratory of Special Functional Aggregated Materials, Ministry of Education; School of Chemistry and Chemical Engineering, Shandong University, Jinan, 250100, P. R. China.

Abstract: Highly biocompatible near-infrared-emitting CdSeTe alloyed quantum dots (QDs) were fabricated in aqueous medium with octa-aminopropyl polyhedral oligomeric silsesquioxane (OA-POSS) as the capping agent. By changing the size and composition of CdSeTe alloyed QDs the fluorescence emission peak reached to near infrared (NIR) region (681 nm) with photoluminescent quantum yield (QY) of 26.4%. POSS-CdSeTe QDs were prepared by conjugating OA-POSS to CdSeTe QDs through condensation reaction utilizing EDC. And the optical properties of CdSeTe QDs were retained with improved biocompatibility. Furthermore, the as-prepared NIR-emitting POSS-CdSeTe alloyed QDs have been successfully applied to SiHa cell imaging, which demonstrates their promising applications in biomedical field.

Key words: NIR-emitting CdSeTe QDs, OA-POSS, high biocompatibility, water-soluble, cell-imaging

1. Introduction

Quantum dots (QDs) offer several significant advantages over organic dyes, including size-tunable photoluminescence spectra, narrow and symmetric emission spectra, broad excitation spectra, high photoluminescent quantum yields and resistance against photobleaching.[1-3] These properties make QDs ideal candidates for

biological labeling and imaging. The near-infrared-emitting QDs between 650 and 900 nm are of particular interest for biological applications because biological autofluorescence and absorbance can be reduced to their minima in this wavelength range. This allows penetration of excitation and fluorescence photons deep into biological samples with reduced interaction and photodamage to the surrounding tissues.[4,5]

Generally, the CdTe QDs of 7 nm can reach to 720 nm in emission, while the big QDs size is not favorable for biological applications.[6] The CdSe-based QDs can only reach 650 nm in emission, which just falls short of the optimal near-infrared range.[7] The syntheses of type-II core-shell QDs (e.g. CdTe/CdSe, CdSe/ZnTe and CdTe/CdSe/ZnS) or alloyed QDs (e.g. CdSeTe, CdSTe and CdHgTe) are good ways for the preparation of high quality NIR-emitting QDs.[8-12] The CdSeTe alloyed QDs have a nonlinear effect between the band-edge emission and composition. This nonlinear effect leads to new optical properties which are not available from the parent binary QDs.

Bailey and Nie reported for the first time the synthesis of NIR-emitting CdSeTe QDs in organometallic route.[10] They tuned the quantum emission wavelength without changing the particle size and the as-prepared CdSeTe QDs were successfully applied in cell labeling.[13] Afterwards, CdSeTe/CdS core-shell QDs were synthesized in organometallic route and were applied in HeLa cell imaging.[14] Water-soluble CdSeTe/CdS core-shell QDs for in vivo imaging were prepared by surface modification of hydrophobic QDs with bifunctional thiol ligands.[15] The presence of a high-band-gap, oxidation-resistant shell significantly improved the QYs and stability of CdSeTe/CdZnS core/shell QDs, making them promising fluorescence probes for NIR biological imaging.[16] The CdSeTe QDs were successfully incorporated into porous polystyrene microbeads to fabricate NIR-emitting microbeads with low cytotoxicity, which were coupled with goat anti-mouse IgG and applied in multiplexed bioassays.[17]

Although conspicuous progresses have been made in the synthesis of NIR emitting CdSeTe QDs through organometallic routes, the aqueous synthesis route for

QDs is relatively simpler, cheaper, less toxic and more environment-friendly. Also the resulting QDs are water-soluble, which make them convenient for the biological applications. Rogach demonstrated a successful synthesis of water soluble alloyed CdSeTe nanocrystals stabilized with TGA in aqueous system.[18] But the optical properties of the synthesized QDs were poor and need to be improved. The microwave synthesis method can be applied to prepare alloyed CdSeTe QDs with high photoluminescence (PL) quantum yields.[19] A facile method is developed for the preparation of water-soluble NIR-emitting CdSeTe alloyed QDs with L-cysteine as the capping agent. The as-prepared QDs were applied for cell imaging and biosensing.[20,21] The CdSeTe/ZnS and CdSeTe/CdS/ZnS core-shell QDs with high compatibility were synthesized and were used for ultrasensitive immunoassay.[6,22] However, synthesizing core-shell QDs involves relatively complicated preparation process and may lead to a drastic increase in QDs size. Alternatively, QDs coated by stable and nontoxic capping ligands can obtain good biocompatibility and also retain their unique photophysical properties.[23]

Recently, polyhedral oligomeric silsesquioxane (POSS) has attracted much interest in materials field due to its unique structure.[24-26] POSS exhibits high stability and excellent biocompatibility under biological environment[27,28] and has shown great potential in tissue engineering for clinical applications.[29-33] Octa-aminopropyl POSS (OA-POSS) is a subtype of POSS with eight amine groups (-NH_2) rendering it a desirable and versatile candidate for further modifications. It is ideal for reactions with carboxyl groups (-COOH) that exist on QDs to form strong covalent bonds through cross-linking reagents. It is a simple procedure for coating OA-POSS on surface of the QDs to render them biocompatible and their eventual small sizes are favorable in biomedical applications. Currently, several studies about the composites of POSS and QDs were reported involving DNA optosensing,[34] photosensitizers of solar cells[35] and cell imaging,[26,36,37] in which visible emitting CdTe or CdSe QDs were used. To the best of our knowledge, near-infrared-emitting POSS-modified QDs have not been synthesized up to now.

Herein, we report the preparation of NIR-emitting CdSeTe alloyed QDs in

aqueous solution using OA-POSS as the capping agent. OA-POSS was applied to improve the biocompatibility of the CdSeTe QDs. MTT assay method was applied to evaluate the cytotoxicity of the as-prepared QDs. SiHa cells incubated with POSS-CdSeTe QDs exhibited higher cell viability than the CdSeTe QDs. The POSS-CdSeTe QDs were successfully applied in cellular imaging.

2. Experimental section

2.1 Materials

Cadmium chloride ($CdCl_2 \cdot 2.5H_2O$), potassium borohydride (KBH_4), sodium tellurite (Na_2TeO_3), sodium selenite (Na_2SeO_3) and sodium hydroxide (NaOH) were purchased from Sinopharm Chemical Reagent Co. Ltd. N-acetyl-L-cysteine (NAC), 1-ethyl-3-[3-dimethylaminopropyl] carbodiimide hydrochloride (EDC), 3-(4,5-dimethylthiazol-2-yl)-2,5-diphenyltetrazolium bromide (MTT) were purchased from Sigma-Aldrich Chemical Co. Octa-aminopropyl polyhedral oligomeric silsesquioxane (OA-POSS) was provided by the School of Chemistry and Chemical Engineering of Shandong University.[38,39] All chemicals were of analytical reagent grade and were used without further purification. Ultra pure water (18.2 MΩ·cm) was used throughout the experiment.

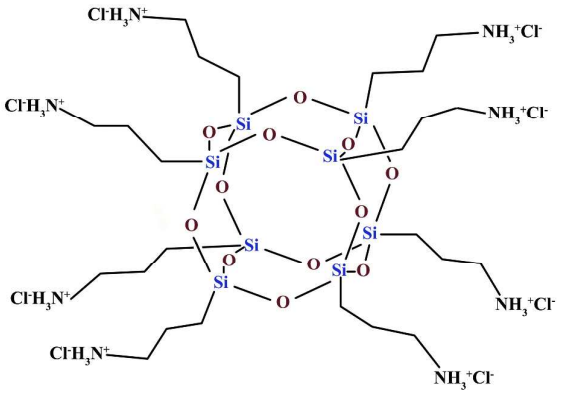

Fig. 1 Structure of OA-POSS as used in the experiment.

2.2 Synthesis and purification of N-acetyl-L-cysteine (NAC) capped CdSeTe QDs

In a typical synthesis, 0.6 mmol NAC was dissolved in 40 mL ultrapure water in a three necked vessel under magnetic stirring. Then 0.5 mmol $CdCl_2 \cdot 2.5H_2O$ was

added and stirred at room temperature. Different molar ratios of Na_2TeO_3 and Na_2SeO_3 were mixed in ultrapure water used as Te and Se precursors. After stirring for 30 min, an excess amount of KBH_4 and 0.1 mmol the Na_2TeO_3 and Na_2SeO_3 mixture were added into the above solution. The solution pH was adjusted with an appropriate amount of 1 M NaOH solution. The reaction mixture was heated to 100 □ and refluxed for varied times with a condenser attached to obtain CdSeTe QDs of different sizes. In order to remove the unreacted species and by-products, the as-prepared QDs were precipitated and washed with ethanol by centrifugation. The purified QDs were dried in vacuum at 40 □ overnight.

2.3 Synthesis and purification of OA-POSS modified CdSeTe QDs

The CdSeTe QDs prepared above were conveniently conjugated to OA-POSS using EDC as a coupling reagent. The concentration of the as-prepared CdSeTe QDs is calculated according to Peng's method.[40] Appropriate amount of EDC was mixed with the CdSeTe QDs solution in a flask and activated at room temperature for 30 min. Then OA-POSS was added to the flask and stirred for 4 h. The molar ratio of CdSeTe QDs, EDC and OA-POSS was fixed at 1:5000:10. After the modification of OA-POSS on CdSeTe QDs, the product was purified as described above. The CdSeTe QDs coupling with and without OA-POSS were separately defined as POSS-CdSeTe QDs and CdSeTe QDs throughout the article.

2.4 Cytotoxicity assay

The human cervical tumor cell line SiHa were applied to evaluate the cytotoxicity of the POSS-CdSeTe QDs and CdSeTe QDs with MTT assay.[41] The detailed process was described in our previous report.[42] In this paper the concentrations of the POSS-CdSeTe QDs and CdSeTe QDs were 1.25, 5, 10, 15, 20, 40, 60, 80 and 100 μg mL^{-1} and the incubation time for SiHa cells was 24 h.

2.5 Cell labeling with the POSS-CdSeTe QDs and CdSeTe QDs

SiHa cells were cultured in DMEM supplemented with 10% fetal bovine serum in a 5% CO_2 incubator at 37 □. The cells were grown overnight in a 24 well plate, in which each well contained sterile glass coverslips. After removing the medium by washing three times with PBS solution, cells were incubated with the as-prepared

POSS-CdSeTe QDs and CdSeTe QDs at concentration of 60 μg mL^{-1} for 24 h. In vitro fluorescence imaging was then carried out after washing cells with the PBS buffer solution.

Confocal fluorescence images of the stained cells were obtained with Olympus FV-300 laser scanning confocal microscope with a 40× water-immersion objective lens (N.A. = 1.25). Cells were imaged using an excitation wavelength of 488 nm from an Ar^+ laser and a 570 nm bandpass filter in the detection channel.

2.6 Apparatus and characterization of samples

The pH values of solution were measured with a Sartorius PB-10 pH meter. UV-visible absorption spectra were collected on a UV-2550 spectrophotometer at room temperature. Fluorescence experiments were performed on a Hitachi F-4500 fluorescence spectrophotometer using an excitation wavelength of 400 nm. X-ray powder diffraction (XRD) analysis was conducted on a Bruker D8 Advance X-ray diffractometer (Cu K_α radiation (λ = 1.54178 Å)). Transmission electron microscopy (TEM) images were obtained with a JEOL JEM-2100F transmission electron microscope operating at an acceleration voltage of 200 kV. Fourier transform infrared spectra (FTIR) were obtained on a Nicolet FTIR760 spectrometer. The energy dispersive X-ray spectra (EDS) were conducted on a HORIBA EMAX Energy EX-450 energy dispersive X-ray spectrometer. The electrophoretic mobility (Zeta potential) of the as-prepared QDs was measured by Zetapals (Brookhaven Instruments Corp, USA). The dynamic light scattering (DLS) experiments were performed on a BI-200SM dynamic and static light scattering instrument (Brookhaven Instruments Corp, USA). The absolute PL efficiency of the as-prepared POSS-CdSeTe QDs was determined by Edinburgh FS-920 fluorescence spectrometer equipped with integrating sphere system.

3. Results and discussion

The near-infrared-emitting CdSeTe alloyed quantum dots (QDs) capped with N-acetyl-L-cysteine (NAC) were synthesized in aqueous media. The as-prepared QDs were precipitated and washed with ethanol by centrifugation in order to remove the

unreacted species and by-products. The growth rate of CdSeTe QDs is fast under optimal conditions and the emission peak wavelength of CdSeTe QDs shifts to 681 nm after reactions of 4 h. OA-POSS is a subtype of POSS with eight amine groups ($-NH_2$) rendering it a desirable and versatile candidate for further modifications with carboxyl groups (-COOH) that exist on NAC-capped CdSeTe QDs to form strong covalent bonds. The CdSeTe alloyed QDs prepared above were conveniently conjugated to OA-POSS using EDC as a coupling reagent, and then the highly biocompatible near-infrared-emitting POSS-CdSeTe alloyed QDs were fabricated. The optical properties of CdSeTe QDs were retained with improved biocompatibility after the modification of OA-POSS. The cytotoxicity test was conducted by MTT assay method. Furthermore, the as-prepared NIR-emitting POSS-CdSeTe alloyed QDs have been successfully applied to SiHa cell imaging, which demonstrates their promising applications in biomedical field.

Temporal evolution of UV-visible absorption spectra and normalized PL emitting spectra of the as-prepared CdSeTe QDs are presented in Fig. 2. Both absorption and emission spectra shift to longer wavelength by prolonging the growth time, which is on the basis of quantum-confined size effects. The near-infrared emission CdSeTe QDs can be obtained through prolonging the refluxing time under suitable conditions. The CdSeTe QDs exhibit well-resolved absorption maximum peak shape and symmetrical fluorescent emission peaks, indicating a narrow size distribution. The growth rate of CdSeTe QDs is fast under optimal conditions and the emission peak wavelength of CdSeTe QDs shifts to 681 nm after reactions of 4 h. The band edge emission of CdSeTe QDs achieves at nearly 750 nm with an absolute photoluminescence quantum yield of 26.4%.

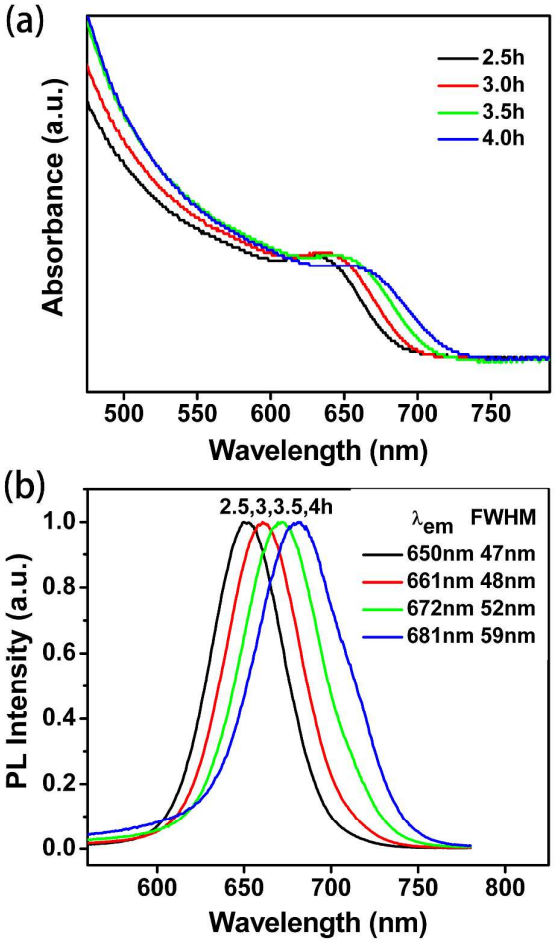

Fig. 2 Temporal evolution of UV-visible absorption spectra (a) and normalized PL emitting spectra (b) of the as-prepared CdSeTe QDs (Cd/Te=10:1, pH=11.75, Se/Te=3:7).

The Te^{2-} and Se^{2-} ions were reduced when KBH_4 and the mixture of Na_2TeO_3 and Na_2SeO_3 were added, just then a large number of nuclei were generated and free Cd and Te (Se) precursor were consumed for the growth of CdSeTe QDs. With the depletion of free Cd and Te (Se) precursor, the CdSeTe QDs growth can only depend on the route of Ostwald ripening, which means the smaller particles dissolved, providing monomers for building the larger ones. It is known that the characteristic of Ostwald ripening is a slow growth rate, resulting in a broadening FWHM (full width at half maximum) as shown in Fig. 2b.[43-45]

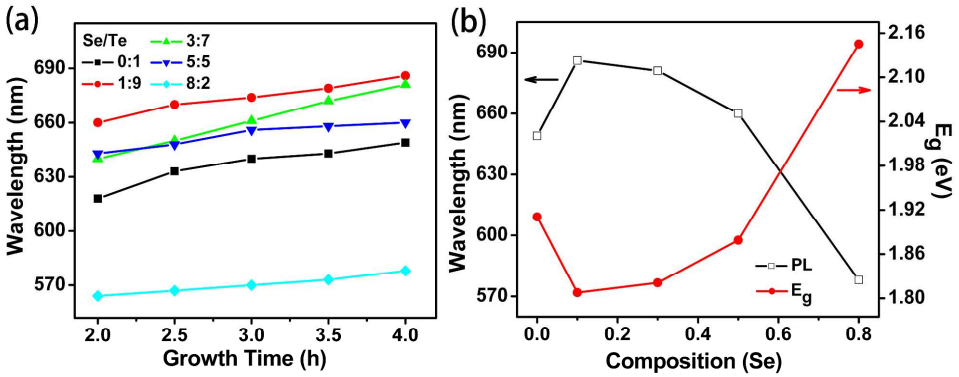

Fig. 3 (a) The relationship between PL wavelength and growth time of the CdSeTe QDs with different Se/Te feed ratios (b) PL wavelength and bandgap (E_g) of CdSeTe QDs (with 4 h growth time) as a function of Se/Te feed ratios.

To investigate the relationship between composition and optical properties of the as-prepared CdSeTe QDs, different compositions of NAC-capped CdSeTe alloyed QDs were synthesized by controlling different feed ratios of Se to Te with the same reaction time as shown in Fig. 3a. Compared with binary CdTe QDs, the CdSeTe alloyed QDs shift obviously to longer wavelength with the incorporation of Se ions. The growth rate decreases when the Se/Te feed ratio is 8:2, in which case the structure of CdSeTe QDs is similar to the CdSe QDs. The CdSe QDs have a wider band gap (1.74 eV) than CdTe QDs (1.45 eV), leading to the blue shift of emitting wavelength for CdSeTe QDs. The PL wavelength and bandgap (E_g) of the CdSeTe QDs (with 4 h growth time) reveals an obvious nonlinear relationship with the varied compositions (Se) as shown in Fig. 3b. It is safe to say that this nonlinear relationship leads to the unusually large spectral shifts in Fig. 3a. The CdSeTe alloyed QDs with Se compositions of 10% and 30% show faster growth rate under the same synthetic conditions, demonstrating larger redshift of the emitting towards longer wavelengths in contrast to the parent CdTe and CdSe QDs. The PL wavelengths of CdSeTe QDs with Se/Te feed ratios of 1:9 and 3:7 were gradually closer as time prolonging.

Table 1. The actual composition of CdSeTe QDs with different Se/Te feed ratios.

Sample	Se/Te feed ratio	Actual composition Se/Te
CdTe	0/1	0/1
CdSe(0.1)Te(0.9)	0.1/0.9	0.15/0.85
CdSe(0.3)Te(0.7)	0.3/0.7	0.35/0.65
CdSe(0.5)Te(0.5)	0.5/0.5	0.54/0.46
CdSe(0.8)Te(0.2)	0.8/0.2	0.87/0.13

Table 1 lists the actual compositions of CdSeTe alloyed QDs with different Se/Te feed ratios, which was measured by EDS. The actual Se composition is slightly higher than its feed ratio, which means it is easier for Se^{2-} to nucleate with Cd^{2+} than the Te^{2-} ions. The binding energy of CdSe (1.322±0.26 eV) is higher than that of CdTe (1.036±0.157 eV).[46] On the other hand, the solubility product (K_{sp}) of CdTe ($K_{sp}=1\times10^{-42}$) is much lower than CdSe ($K_{sp}=6.3\times10^{-36}$). The compromised results of binding energy and K_{sp} would ensure the growth rate of CdSe and CdTe to stay at the similar level.

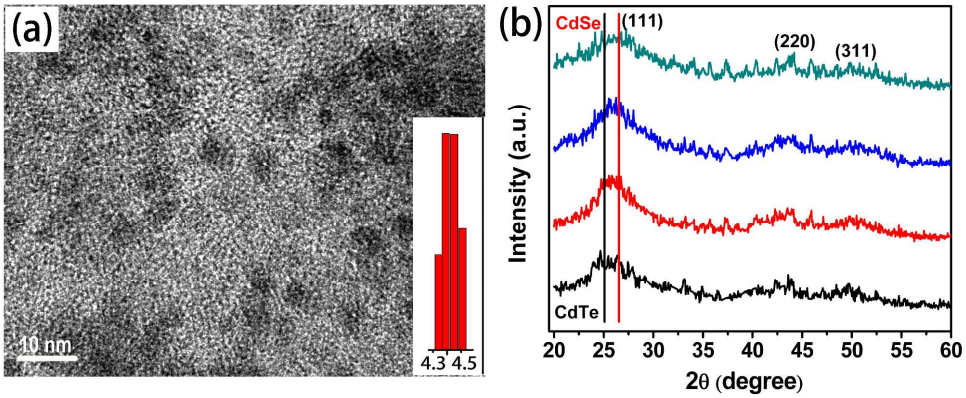

Fig. 4 (a) TEM image of CdSeTe QDs with emission peak of 681 nm (The inset is the histogram of the size distribution of the prepared CdSeTe QDs analyzed by dynamic light scattering (DLS)). (b) XRD patterns of CdSeTe QDs with different Se/Te molar ratios (from the bottom up: CdSeTe(0/1)649, CdSeTe(0.3/0.7)681, CdSeTe(0.5/0.5)660, CdSeTe(0.8/0.2)578).

TEM image of the as-prepared CdSeTe QDs with emission peak wavelength of

681 nm is presented in Fig. 4a. The QDs appear as spherical particles with excellent monodispersity and its particle size is 4.3 nm, which is in good accordance with the DLS analysis result. The powder XRD patterns (Fig. 4b) of CdSeTe alloyed QDs confirm the crystallinity of the cubic (zinc-blende) structure. Three broad diffraction peaks typical for nanoparticles[47] appear at (111), (220) and (311). The XRD diffraction peaks for all CdSeTe QDs shift towards the values of bulk CdSe as Se composition increased, suggesting a transformation from CdTe lattice to CdSe during the formation of the alloyed QDs.

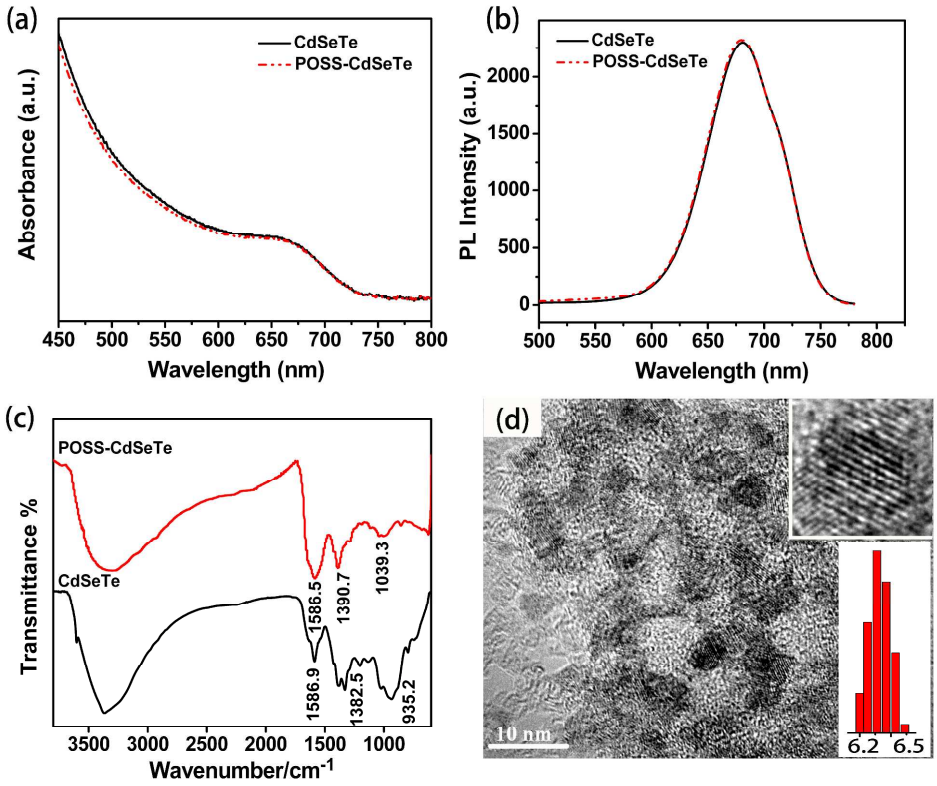

Fig. 5 UV-visible absorption spectra (a) and PL spectra (b) of CdSeTe QDs with emission peak of 681 nm before and after the modification of OA-POSS (c) FTIR spectra of the CdSeTe QDs and POSS-CdSeTe QDs (d) TEM image of the OA-POSS modified CdSeTe QDs (The insets are HRTEM image and DLS analysis result of the POSS-CdSeTe QDs).

The OA-POSS were conjugated to CdSeTe QDs using EDC as activating agent. OA-POSS is a subtype of POSS with eight amine groups (-NH_2) rendering it a

desirable and versatile candidate for further modifications with carboxyl groups (-COOH) that exist on NAC-capped CdSeTe QDs to form strong covalent bonds. UV-visible absorption spectra and PL emission spectra of the CdSeTe QDs before and after the modification of OA-POSS are presented in Fig. 5a and Fig. 5b. The absorption and PL emitting wavelength of CdSeTe QDs remain unchanged after conjugation with OA-POSS, which means the modification of OA-POSS has no effects on the optical properties of CdSeTe QDs. FTIR analysis was applied to confirm successful coating of the CdSeTe QDs with OA-POSS as shown in Fig. 5c. Compared with CdSeTe QDs, POSS-CdSeTe QDs show a new peak at 1039.3 cm^{-1} arising from variable strong stretching vibrations of the Si-O-Si bonds in the OA-POSS.[26] The electrophoretic mobility (Zeta potential) of the as-prepared CdSeTe QDs and POSS-CdSeTe QDs was measured separately as -11.59 mV and 12.12 mV, which further confirm the surface coating of OA-POSS on the CdSeTe QDs. TEM and HRTEM images of the POSS-CdSeTe QDs with emission peak wavelength of 681 nm are presented in Fig. 5d. The highly crystalline CdSeTe cores of the POSS-CdSeTe QDs have a mean diameter of 4.3 nm. OA-POSS coating can't be exhibited in TEM images due to its amorphous structure. In DLS analysis, the mean diameter of POSS-CdSeTe QDs increases to about 6.3 nm, indicating successful coating of OA-POSS on the CdSeTe QDs.

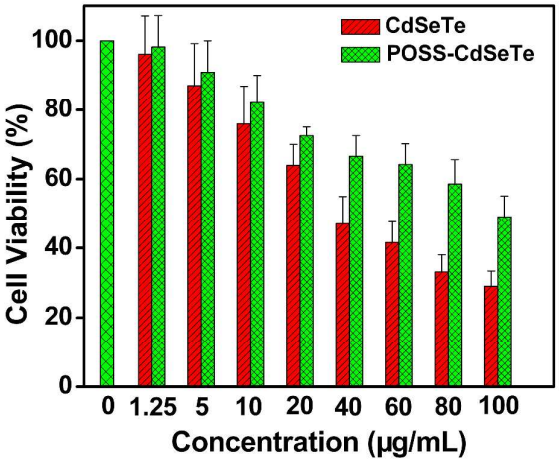

Fig. 6 Cytotoxicity of SiHa cells incubated with different concentrations of POSS-CdSeTe QDs and CdSeTe QDs for 24 h.

The cytotoxicity of QDs has been paid close attention by many researchers, since it is a critical characteristic for their further biological applications. It is generally acknowledged that the leakage of toxic Cd^{2+} ions from QDs and the tendency of QDs to aggregate in living cells are the two significant factors that lead to their cytotoxicity.[48-51] So far, synthesizing core-shell QDs structure, surface coating of photostable and biocompatible materials and incorporation of nontoxic ions are effective strategies to reduce the cytotoxicity of QDs.[36,42,52,53] Herein, OA-POSS was employed as a kind of stable and biocompatible capping agent to render CdSeTe QDs better biocompatibility. The cellular response to QDs was examined using MTT assay method. The cytotoxicity effects of POSS-CdSeTe QDs and CdSeTe QDs were studied on SiHa cells at various concentrations for 24 h as is shown in Fig. 6. A significant dose-dependent phenomenon in cellular viability is observed. There is no obvious suppression of cell viability with low concentrations of QDs. By comparison, POSS-CdSeTe QDs were significantly less toxic than CdSeTe QDs at all dosages. The cell viability for POSS-CdSeTe QDs at concentration of 100 μg mL^{-1} is about 50%, while it is less than 30% for CdSeTe QDs, indicating a significant increase in the biocompatibility of POSS-CdSeTe QDs. Although the diameter of CdSeTe QDs increases with the OA-POSS coating, the quantities of CdSeTe QDs and POSS-CdSeTe QDs ingested by SiHa cells are nearly the same as shown in Fig. 7. The POSS-CdSeTe QDs have a surface coating with both hydrophilic and hydrophobic moieties, which allows rapid intracellular uptake across the lipophilic cell membranes.[54] The encapsulation of CdSeTe QDs with OA-POSS reduces the cytotoxicity compared to CdSeTe QDs since the release of Cd^{2+} was effectively inhibited. In addition, OA-POSS is nontoxic and photostable, which can protect the QDs from aggregating caused by photobleaching.

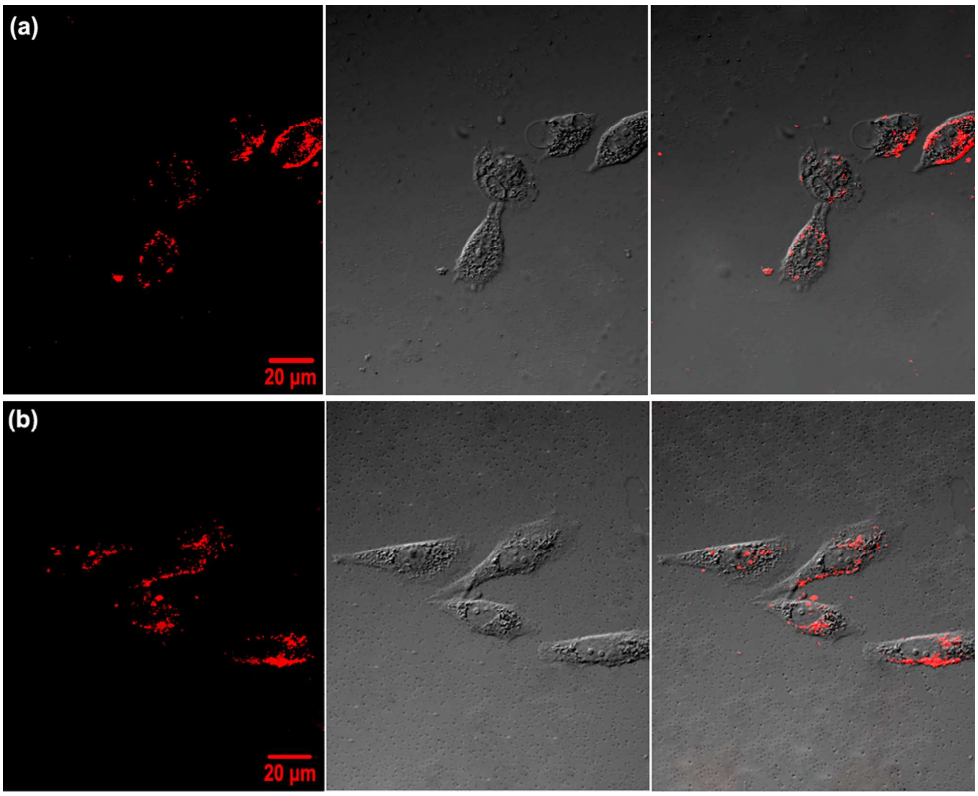

Fig. 7 Laser scanning confocal microscopy images (left: confocal fluorescence images, middle: differential interference contrast (DIC) images, right: overlay of the left and middle rows) of SiHa cells incubated with CdSeTe QDs (a) and POSS-CdSeTe QDs (b) at concentration of 60 μg mL^{-1} for 24 h.

The cancer cell lines can be labeled with quantum dots by membrane rupturing on nonspecific bindings or receptor mediated endocytosis.[55-57] After being incubated by 60 μg mL^{-1} of POSS-CdSeTe QDs and CdSeTe QDs for 24 h, the uptake of QDs in SiHa cells is shown according to laser scanning confocal imaging. It is demonstrated in Fig. 7 that POSS-CdSeTe QDs can be successfully internalized into cells via endocytosis and show red punctuated fluorescence around the nucleus. No fluorescence signal was measured for SiHa cells without the incubation of QDs, indicating that the red fluorescence originate from the QDs. More importantly, no sign of morphological damage to the cells is observed upon incubation with the POSS-CdSeTe QDs, while cells incubated with CdSeTe QDs were significantly damaged under the same conditions. In our previous report, visible emitting

POSS-CdTe QDs were applied in SiHa and MC3T3-E1 cell labeling. And the POSS-CdTe QDs exhibited better biocompatibility than CdTe QDs[54]. Based on our study we think that the surface modification of QDs by POSS is a feasible strategy to make the as-prepared QDs more biocompatible for cellular studies.

Conclusions

In summary, the octa-aminopropyl polyhedral oligomeric silsesquioxane (OA-POSS) coated near-infrared-emitting CdSeTe alloyed quantum dots with low toxicity were fabricated in aqueous system. The emission wavelengths of the alloyed CdSeTe quantum dots can be tuned by changing composition and size, in which a nonlinear relationship exists between the band gap and composition. OA-POSS and CdSeTe quantum dots were conjugated together through condensation reaction. The as-prepared POSS-CdSeTe quantum dots obtained improved biocompatibility and retained the unique photophysical properties of CdSeTe quantum dots. The cytotoxicity results revealed that the cytotoxic effect of CdSeTe quantum dots towards living cells was dramatically reduced with the surface capping of OA-POSS. The usage of near-infrared-emitting POSS-CdSeTe quantum dots in biological applications gave low interference with biomolecules in this region. For preliminary cell labeling application, the favorable biocompatibility of OA-POSS modified CdSeTe quantum dots was demonstrated by using SiHa cells with laser scanning confocal microscopy. The POSS-CdSeTe quantum dots were internalized into cells via endocytosis and showed no sign of morphological damage to the SiHa cells, indicating that the near-infrared-emitting POSS-CdSeTe alloyed quantum dots are highly promising fluorescent labels in biomedical field.

Acknowledgments

This work was financially supported by NSFC (Contract No. 51321091, 21274081) and IIFSDU.

References

1 V. I. Klimov, *Los Alamos Science*, 2003, **28**, 214-220.

2 I. L. Medintz, H. T. Uyeda, E. R. Goldman and H. Mattoussi, *Nature Materials*,

2005, **4**, 435-446.

3 E. R. Goldman, I. L. Medintz and H. Mattoussi, *Anal. Bioanal. Chem.*, 2006, **384**, 560-563.

4 Y. T. Lim, S. Kim, A. Nakayama, N. E. Stott, M. G. Bawendi and J. V. Frangioni, *Mol. Imaging*, 2003, **2**, 50-64.

5 A. L. Rogach, A. Eychmuller, S. G. Hickey and S. V. Kershaw, *Small*, 2007, **3**, 536-557.

6 G. X. Liang, L. L. Li, H. Y. Liu, J. R. Zhang, C. Burda and J. J. Zhu, *Chem. Commun.*, 2010, **46**, 2974-2976.

7 R. C. Somers, M. G. Bawendi and D. G. Nocera, *Chem. Soc. Rev.*, 2007, **36**, 579-591.

8 P. Reiss, M. Protiere and L. Li, *Small*, 2009, **5**, 154-168.

9 W. J. Zhang, G. J. Chen, J. Wang, B. C. Ye and X. H. Zhong, *Inorg. Chem.*, 2009, **48**, 9723-9731.

10 R. E. Bailey and S. M. Nie, *J. Am. Chem. Soc.*, 2003, **125**, 7100-7106.

11 B. Xue, D. W. Deng, J. Cao, F. Liu, X. Li, W. Akers, S. Achilefu and Y. Q. Gu, *Dalton Trans.*, 2012, **41**, 4935-4947.

12 H. F. Qian, C. Q. Dong, J. L. Peng, X. Qiu, Y. H. Xu and J. C. Ren, *J. Phys. Chem. C*, 2007, **111**, 16852-16857.

13 R. E. Bailey, J. B. Strausburg and S. M. Nie, *J. Nanosci. Nanotech*, 2004, **4**, 569-574.

14 W. Jiang, A. Singhal, J. N. Zheng, C. Wang and W. C. W. Chan, *Chem. Mater.*, 2006, **18**, 4845-4854.

15 T. Jin, F. Fujii, Y. Komai, J. Seki, A. Seiyama and Y. Yoshioka, *Int. J. Mol. Sci.*, 2008, **9**, 2044-2061.

16 T. Pons, N. Lequeux, B. Mahler, S. Sasnouski, A. Fragola and B. Dubertet, *Chem. Mater.*, 2009, **21**, 1418-1424.

17 B. Xing, W. W. Li, X. B. Wang, H. J. Dou, L. Wang, K. Sun, X. T. He, J. S. Han, H. S. Xiao, J. M. Miao and Y. Li, *J. Mater. Chem.*, 2010, **20**, 5664-5674.

18 N. Piven, A. S. Susha, M. Doblinger and A. L. Rogach, *J. Phys. Chem. C*, 2008,

112, 15253-15259.

19 L. X. Song, J. L. Duan and J. H. Zhan, *Mater. Lett.*, 2010, **64**, 1843-1845.

20 G. X. Liang, M. M. Gu, J. R. Zhang and J. J. Zhu, *Nanotechnology*, 2009, **20**, 415103.

21 G. X. Liang, H. Y. Liu, J. R. Zhang and J. J. Zhu, *Talanta*, 2010, **80**, 2172-2176.

22 L. L. Li, Y. Chen, Q. Lu, J. Ji, Y. Y. Shen, M. Xu, R. Fei, G. H. Yang, K. Zhang, J. R. Zhang and J. J. Zhu, *Scientific Reports*, 2013, **3**, 1529.

23 A. F. E. Hezinger, J. Tessmar and A. Gopferich, *Eur. J. Pharm. Biopharm.*, 2008, **68**, 138-152.

24 D. B. Cordes, P. D. Lickiss and F. Rataboul, *Chem. Rev.*, 2010, **110**, 2081-2173.

25 G. Z. Li, L. C. Wang, H. L. Ni and C. U. Pittman, *J. Inorg. Organomet. Polym.*, 2001, **11**, 123-154.

26 S. B. Rizvi, L. Yildirimer, S. Ghaderi, B. Ramesh, A. M. Seifalian and M. Keshtgar, *Int. J. Nanomedicine.*, 2012, **7**, 3915-3927.

27 F. F. Du, H. Wang, Y. Y. Bao, B. Liu, H. T. Zheng and R. K. Bai, *J. Mater. Chem.*, 2011, **21**, 10859-10864.

28 H. Ghanbari, B. G. Cousins and A. M. Seifalian, *Macromol. Rapid Commun.*, 2011, **32**, 1032-1046.

29 P. Jungebluth, E. Alici, S. Baiguera, K. Le Blanc, P. Blomberg, B. Bozoky, C. Crowley, O. Einarsson, K. H. Grinnemo, T. Gudbjartsson, S. Le Guyader, G. Henriksson, O. Hermanson, J. E. Juto, B. Leidner, T. Lilja, J. Liska, T. Luedde, V. Lundin, G. Moll, B. Nilsson, C. Roderburg, S. Stromblad, T. Sutlu, A. I. Teixeira, E. Watz, A. Seifalian, P. Macchiarini, *Lancet*, 2011, **378**, 1997-2004.

30 S. S. Suri, H. Fenniri and B. Singh, *J. Occup. Med. Toxicol.*, 2007, **2**, 16.

31 R. Verdejo, G. Jell, L. Safinia, A. Bismarck, M. M. Stevens and M. S. Shaffer, *J. Biomed. Mat. Res. Part A.*, 2009, **88**, 65-73.

32 M. Ahmed, H. Ghanbari, B. G. Cousins, G. Hamilton and A. M. Seifalian, *Acta Biomaterial.*, 2011, **7**, 3857-3867.

33 M. Desai, R. Bakhshi, X. Zhou, M. Odlyha, Z. You, A. M. Seifalian and G. Hamilton, *J. Endovascul. Therap.*, 2012, **19**, 415-427.

34 Y. He, H. F. Wang and X. P. Yan, *Chem. Eur. J.*, 2009, **15**, 5436-5440.

35 Y. Wang, A. Vaneski, H. H. Yang, S. Gupta, F. Hetsch, S. V. Kershaw, W. Y. Teho, H. R. Li and A. L. Rogach, *J. Phys. Chem. C*, 2013, **117**, 1857-1862.

36 G. Brakmane, S. Y. Madani and A. M. Seifalian, *Anti-Cancer. Agents. Med. Chem.*, 2013, **13**, 821-832.

37 S. Ghaderi, B. Ramesh and A. M. Seifalian, *J. Nanosci. Nanotechnol.*, 2012, **12**, 4928-4935.

38 H. Z. Liu, W. A. Zhang and S. X. Zheng, *Polymer*, 2005, **46**, 157-165.

39 F. J. Feher and K. D. Wyndham, *Chem. Commun.*, 1998, **3**, 323-324.

40 W. W. Yu, L. H. Qu, W. Z. Guo and X. G. Peng, *Chem. Mater.*, 2003, **15**, 2854-2860.

41 T. Mosmann, *J. Immunol. Methods*, 1983, **65**, 55-63.

42 J. Du, X. L. Li, S. J. Wang, Y. Z. Wu, X. P. Hao, C. W. Xu and X. Zhao, *J. Mater. Chem.*, 2012, **22**, 11390-11395.

43 S. J. Park, S. Kim, S. Lee, Z. G. Khim, K. Char and T. Hyeon, J. Am. Chem. Soc., 2000, **122**, 8581-8582.

44 D. V. Talapin, S. Haubold, A. L. Rogach, A. Kornowski, M. Haase and H. Weller, *J. Phys. Chem. B*, 2001, **105**, 2260-2263.

45 X. Peng, J. Wickham and A. P. Alivisatos, *J. Am. Chem. Soc.*, 1998, **120**, 5343-5344.

46 Y. Y. Xia, *Handbook for Chemical Laboratories,* Chemical industry press, Beijing, 2008.

47 X. H. Zhong, Y. Y. Feng, W. F. Knoll and M. Y. Han, *J. Am. Chem. Soc.*, 2003, **125**, 13559-13563.

48 V. A. Sianni, D. S. Koktysh, B. G. Yun, R. L. Matts, T. C. Pappas, M. Motamedi, S. N. Thomas and N. A. Kotov, *Nano Lett.*, 2003, **3**, 1177-1182.

49 A. M. Derfus, W. C. W. Chan and S. N. Bhatia, *Nano Lett.*, 2004, **4**, 11-18.

50 A. Hoshini, K. Fujioka, T. Oku, M. Suga, Y. F. Sasaki, T. Ohta, M. Yasuhara, K. Suzuki and K. Yamamoto, *Nano Lett.*, 2004, **11**, 2163-2169.

51 C. Kirchner, T. Liedl, S. Kudera, T. Pellegrino, A. M. Javier, H. E. Gaub, S. Stolzle,

N. Fertig and W. J. Parak, *Nano Lett.*, 2005, **5**, 331-338.

52 Y. F. Liu and J. S. Yu, *J. Colloid Interface Sci.*, 2010, **351**, 1-9.

53 B. H. Dong, L. X. Cao, G. Su, W. Liu, H. Qu and D. X. Jiang, *J. Colloid Interface Sci.*, 2009, **339**, 78-82.

54 X. Zhao, S. J. Wang, W. J. Zhang, J. C. Qiu, Y. Z. Wu, H. Z. Liu, C. W. Xu and X. P. Hao, *RSC Adv.*, 2014, **4**, 598-604.

55 L. W. Zhang and N. A. Monteiro-Riviere, *Toxicol. Sci.*, 2009, **110**, 138-155.

56 Y. Williams, A. Sukhanova, M. Nowostawska, A. M. Davies, S. Mitchell, V. Oleinikov, Y. Gun'ko, I. Nabiev, D. Kelleher and Y. Volkoy, *Small*, 2009, **5**, 2581-2588.

57 S. Hussain, N. Won, J. Nam, J. Bang, H. Chung and S. Kim, *ChemPhysChem*, 2009, **10**, 1466-1470.

Table of contents

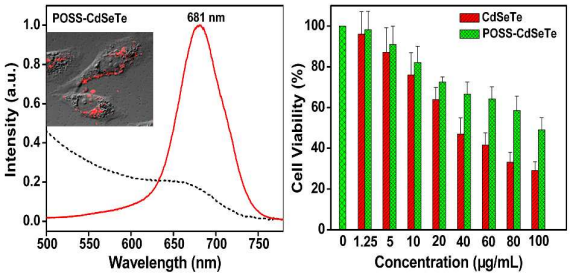

Highly biocompatible near-infrared-emitting OA-POSS modified CdSeTe QDs were fabricated in aqueous and were successfully applied to SiHa cell imaging.